

# HEAT TRANSFER IN VERTICAL TUBE EVAPORATORS I\*

By

K. TETTAMANTI and H. HAJDÚ

(Department of Chemical Unit Operations, Technical University, Budapest)

Received April 24, 1972

## I. Apparatus and testing method

### *Introduction*

Boiling equipment in chemical industry: evaporators and distillation reboilers are mostly vertical shell and tube apparatus, in the tubes of which upward flow of the liquid is maintained either by natural circulation (thermosyphon) or by pumping. To design such evaporators, the following data are necessary:

1. The pressure difference (or liquid leg in case of a thermosyphon) required to induce a given flow velocity in the tubes by given heating.

2. The heat transferred by given temperature difference and flow velocity.

Linear velocity is growing continuously along the evaporator tubes in consequence of vapour generation, which implies the variation of flow patterns and of heat transfer intensity too. In vertical tubes the boiling point of the liquid varies also significantly along with the variation of the hydrostatic head. So experimental studies are made 1. either in short tubes where the change in vapour content may be neglected and for design calculations the results are to be integrated along the tube length or 2. in tubes of full industrial length, but the results of such experiments hold only within the conditions investigated.

The design of boiler tubes on purely theoretical basis is not yet possible.

Present work describes an apparatus and experimental method for the determination of the mean heat transfer coefficient in the operating range of natural and forced circulation vertical tube evaporators used in the chemical industry: in case of small temperature difference and heat flux. The measurement of the heating surface temperature, which is generally needed to determine film coefficients, is avoided since it requires special equipment. The mean wall temperature along the tube and the local fluid temperatures are calculated merely on the basis of the measured temperatures and pressures of the heating steam of the inlet and the exit boiled fluid. These measurements are easily executed on any apparatus, so the described method may be applied for the determination of film coefficients in industrial evaporators.

\* Dedicated to Prof. L. Telegdy Kováts on the occasion of his 70th birthday

### 1.1. Previous investigations

Equipment on similar purpose has already been constructed by some investigators. The experimental model may consist of a single tube, since KIRSCHBAUM [5], as well as AKIN and MCADAMS [1] stated that the heat transfer in vertical tube evaporators was not influenced by the number of tubes. Electric resistance heating used by BORISHANSKI et al. [4] is very convenient for experiments, because the transferred heat can be measured exactly with the electric power, but it has the disadvantage of producing a constant heat flux along the tube independently of the flow conditions and that the wall temperature varies at the same time, which is not the case for the steam-heated evaporators of the chemical industry. For this reason KIRSCHBAUM and co-workers [6] as well as BOARTS, BADGER and MEISENBURG [3] used steam heating and determined the transferred heat from the amount of condensed steam. The liquid temperature in the tube was measured by a thermocouple travelling in the tube axis, the temperature of the heating surface was evaluated from readings of several thermocouples placed in wells or borings in the tube wall on the steam side, taking the thickness and the conductivity of the wall into consideration. For these experiments thick wall copper tubes were used *a*) to place the borings *b*) to reduce errors of the obtained surface temperature due to uncertainty in the position of the thermocouple joints. The thermocouples must not be inserted on the boiling side, because it would disturb the boiling and the bubble formation just at the point of measurement. The above experiments furnished a mean film coefficient along the tube (since the local heat flux was unknown) with the integral mean of the temperature difference between the surface and the boiled liquid

$$\bar{q} = \bar{\alpha}_F (\bar{t}_s - \bar{t}_F) = \bar{\alpha}_F \bar{\delta t}_F. \quad (1)$$

Local film coefficients were measured only by TOBILEVITSH and ERE-MENKO [8]. These investigators gathered steam condensate separately from tube sections and by this method they could determine local heat fluxes together with local wall and liquid temperatures.

As a result of investigations we have the following picture of the operation of tube evaporators:

The evaporator tube divides into a *preheat section* and a *vaporisation section*. Although liquid enters the bottom of the tube generally at saturation temperature of the vapour chamber, but there is a pressure difference because of the hydrostatic head and the flow pressure loss and in consequence there is an elevation of the boiling point. The length of the preheat section is a function of the flow rate and of the heat flux. In this section there is one phase liquid flow, but this does not determine a heat transfer without change in phase: on surface points where the temperature surpasses the local boiling tempera-

ture, the so-called local boiling is possible even in the preheat section. In this case the mechanism and the coefficient of heat transfer is similar to that of nucleate boiling, but without net vapour formation, because the bubbles growing on the heating surface condense back into the colder liquid core.

Net vapour production begins in the vaporisation section. Here the fluid is at the saturation temperature or superheated by not more than one or two centigrades. The saturation temperature itself decreases upwards in consequence of the pressure drop. Hence a maximum fluid temperature results at the beginning of the vaporisation section. The pressures, the boiling points and the liquid temperatures along the tube were measured by KIRSCHBAUM [6] (Fig. 1).

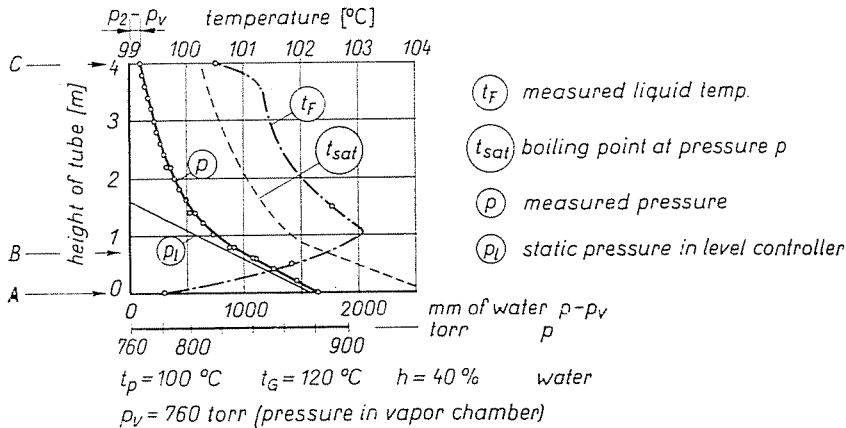


Fig. 1. Pressures and temperatures along the evaporator tube [6]  $t_{sat} = 100^\circ\text{C}$   $t_G = 120^\circ\text{C}$   $h = 40\%$  water  $p_v = 760$  torr (pressure in vapour chamber)  $t_F$  measured liquid temperature;  $t_{sat}$  boiling point at pressure  $p$ ;  $P$  measured pressure;  $p_I$  static pressure in level controller

In the vaporisation section two phase flow patterns change with increasing vapour content. BERENSON and STONE observed for FREON 113 bubble flow up to 0.1 per cent weight of vapour, plug flow for 0.1 to 1.0%, annular flow and transition into mist flow to about 30%. Flow pattern was found to be influenced beside vapour content by mass rate and physical properties of the flow. Heat transfer coefficient is dependent on flow pattern: it has a maximum at the plug-annular flow transition, but falls back to a value near zero in mist flow, the case of heating a gas (the so-called "crisis of heat transfer"). Exit vapour content and flow pattern depend over the tube length on the mass flow rate and the heat flux.

In forced circulation with high flow rate the vaporisation section is often missing, the vapour phase is produced only on the effect of flashing in the vapour chamber.

### 1.2. Experimental equipment

The experimental procedure used by the authors significantly differs from those in previous works in three points:

1. By very careful construction of our apparatus it was possible to determine the transferred heat from both steam- and heated-side heat balance. The standard deviation of the two independent heat balances was  $\pm 1.3\%$ .

2. Direct measurement of the wall temperature was avoided. Its mean value was determined by experimentally checked computation method.

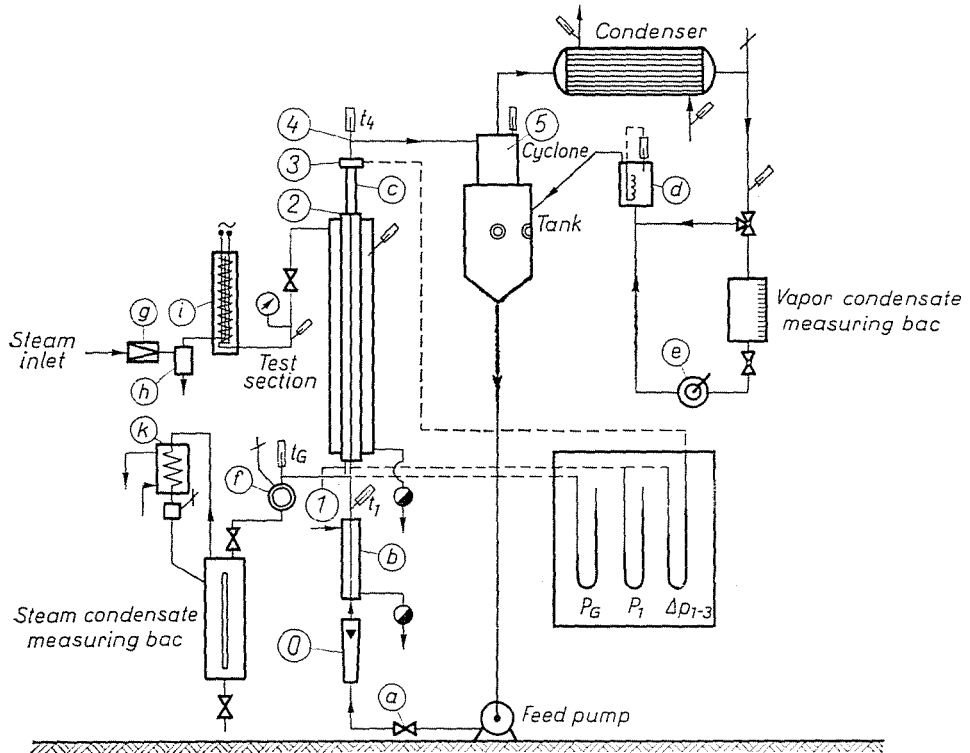


Fig. 2. Overall scheme of equipment: a) feed regulation; b) feed preheater; c) sight section; d) condensate reheater; e) condensate pump; f) condensate level control, vent; g) reducing valve; h) moisture trap; i) steam superheater; k) steam trap

3. Liquid temperature was measured only at the inlet and the exit of the boiler tube. Local values and the real mean temperature were calculated on the basis of heat transfer and pressure drop measurements.

Fig. 2 shows the scheme of the equipment. The steam jacketed boiler tube and the vapour chamber form the evaporator. Dimensions of the evaporator tube are: length 1500 mm, diameter 20/25 mm, material stainless steel KOR 5. Atmospheric and vacuum operation are possible.

Liquid is circulated by a SIHI pump. Flow rate is manually controlled by an angle valve also in the velocity range of natural circulation evaporators.

The test section is preconnected by a preheater and directly followed by a sight section (glass tube of 280 mm length, 20 mm i.d.). During heat transfer measurement the sight glass was coated by heat insulation. The vapour chamber and the connecting vapour line up to the condenser were very carefully insulated against heat loss. The upper part of the vapour chamber is a liquid-vapour separating cyclone, the bottom serves as liquid tank. The vapour was

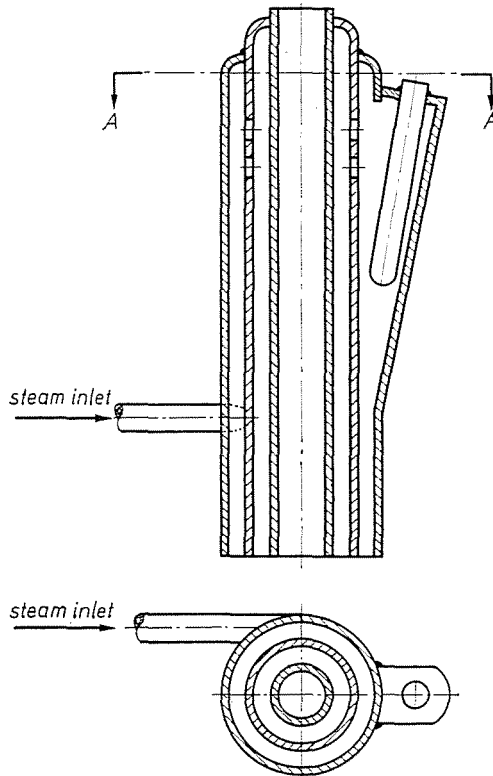


Fig. 3. Upper part of evaporator tube

condensed in the tubes of a shell-and-tube heat exchanger, the condensate was fed back to the liquid tank reheated to the boiling temperature in order to maintain steady state operation.

The heating steam enters the steam jacket after a cyclone droplet separator superheated by 5 to 10 °C in an electric superheater. The steam jacket is double to prevent heat loss of the inner jacket, which is the proper heating jacket. The outside steam jacket is insulating by compensation. Steam enters the outside jacket tangentially to settle out liquid droplets, the top of the parting wall is punched to let the steam pass into the internal jacket and to maintain equal pressure in both steam chambers and by this way prevent heat exchange between them see Fig. 3.

The following measurements were made (see Fig. 2) in the evaporator tube:

at cross  
section

- 0 flow rate of the (here vapour-free) liquid was measured at an accuracy of  $\pm 1\%$  by a calibrated rotameter having 3 floats with 50 to 750 liter/h; 800 to 1500 liter/h; 1500 to 2300 liter/h measuring ranges, respectively;
- 1 at the inlet of the test section temperature ( $t_1$ ) and pressure ( $p_1$ ) of the fluid;
- 2 at the exit from the test section the flow pattern was examined by 1/1000 sec exposure photographs and 500 frame/s motion pictures;
- 3 after the sight section the fluid pressure ( $p_3$ );
- 4 fluid temperature ( $t_4$ );
- 5 in the vapour chamber the temperature ( $t_5$ ) was measured; pressure was equal to atmospheric pressure;
- $w_K$  mass rate of evaporated liquid was determined at  $\pm 2\%$  accuracy in a calibrated 1000 ml measuring tube from the time needed to gather 1000 ml of vapor condensate;
- $w_G$  mass rate of steam condensate (from the internal steam jacket) was determined from the volume of the condensate gathered during 10 min in a calibrated 20 liter vessel aerated through a reflux condenser to prevent flash losses;
- $t_G$  steam condensation temperature near the inlet in the outside steam jacket;
- $p_G$  steam pressure at the bottom of the internal steam jacket.

The temperatures were measured with calibrated mercury thermometers with 0.1 °C scale divisions. Protecting tubes were made from KOR 5 stainless steel of 80 mm length and 10/12 mm diameter, filled with oil, so that the temperature lag due to protecting tubes was less than 0.05 °C.

Pressure gauges were read off mercury filled U-glass manometers with  $\pm 2$  Torr average reading error.

In the course of experiments the state variables of the heating steam and its superheat temperature were controlled constantly, air and steam condensate were continuously removed from the bottom of the steam jacket (latter was checked through the sight-glass).

Readings were made only in steady state operating conditions every 10 minutes, 5 or 6 times in the course of every experiment which lasted 40 to 50 min. For calculations the arithmetic means of the 5 or 6 readings were used. Steady state was verified in the calculations comparing the steam-side and the heated side heat balances.

The transferred heat from the steam-side heat balance:

$$Q_G = w_G \cdot r_G \quad (2)$$

and from the fluid-side balance

$$Q_F = w_{FO} c_F (t_5 - t_1) + w_K r_K \quad (3)$$

Timely variation of  $w_{FO}$ ,  $t_1$ , steam pressure would have caused a discrepancy of the heat fluxes obtained from the two heat balances. For our 66 experiments the mean value of the ratio of the two heat fluxes was  $Q_F/Q_G = 0.996$ , with a standard deviation of  $\pm 0.2\%$ . During operation with small overall temperature difference ( $t_G - t_5 = 5^\circ\text{C}$ ) steady state conditions could hardly be maintained; in these experiments more than 3% discrepancy between  $Q_F$  and  $Q_G$  occurred. In further calculations  $Q_G$  was used.

### 1.3. Evaluation of data

The film coefficient of heat transfer is defined generally by Eq. (1)

$$\frac{Q}{F} = q = \alpha_F (t_s - t_F) \quad (1a)$$

If the film coefficient is a mean along the heating surface, the other quantities in Eq. (1a) should be mean values, too.

When the heat transfer is accompanied by change in phase e.g. in case of nucleate boiling, the mechanism of the transfer and consequently the definition of the film coefficient modifies to

$$q = \alpha_B (t_s - t_{\text{sat}}) \quad (4)$$

where

$t_{\text{sat}}$  is the saturation temperature of the liquid at the actual pressure or its mean value along the tube.

The film coefficients in Eqs (1a) and (4) are identical, if the liquid is at its saturation temperature, but, as we pointed out, this is not always the case for evaporators.

The mean heat flux  $q$  along the tube has been determined from the steam-side heat balance.

The mean wall temperature, liquid temperature and saturation temperature were computed by the method described below.

*1.3.1. Estimation of the true liquid temperature.* The liquid temperature was measured in two cross sections: at 1, inlet of the test section, and at 4 after the exit.

For our computation too, the pressures at these two places were needed, but they were available at 1 and 3. To calculate the heat transfer coefficient, the mean liquid temperature along the test section 1—2 must be known, but at 2 no temperature measurement was possible because of the sight section. The calculation accounts of course for the difference between  $t_2$  and  $t_1$ , and  $p_3$  respectively.

Typical axial temperature and pressure profiles are already known from previous works, e.g. [6], see Fig. 1. In the preheat section liquid temperature is raised until at some tube height it reaches the local boiling point: this is level B (boiling). From this level upwards the fluid temperature is nearly

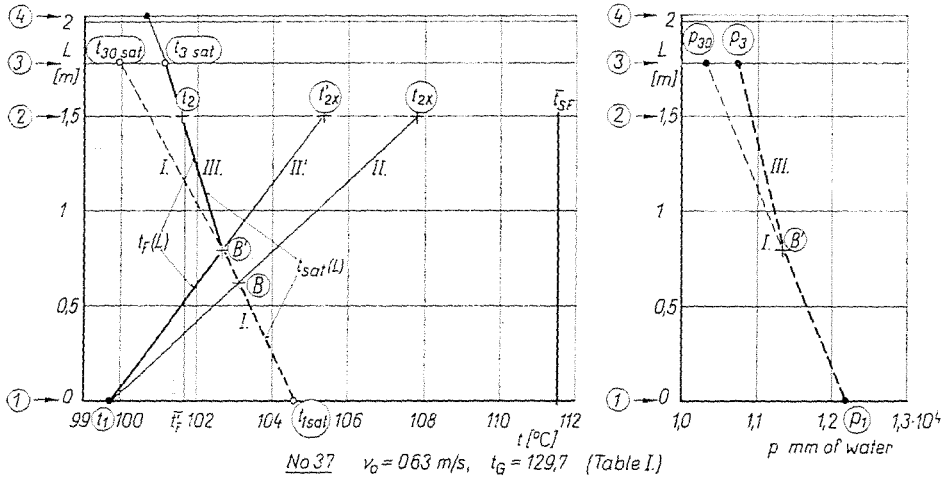


Fig. 4. Determination of  $t_p(L)$  and  $t_{sat}(L)$ : ● Measured values; ○ From steam table; + Calculated values

equal to the local saturation temperature and decreasing with the local pressure. The line of the diminution of the local pressure has a break point at level B due to the apparition of the vapour phase. The local pressure vs.  $L$  can be roughly approximated by two straight lines. In the preheat section its slope  $\frac{dP}{dL}$  is equal to that of one phase liquid flow at the same temperature.

The calculation is performed on the above basis in three steps. It can be represented on the  $t-L$  and the  $p-L$  diagram, Fig. 4.

a) In the  $p-L$  diagram, a straight line representing the preheat section is drawn. Its slope  $\frac{dP}{dL}$  is known from pressure drop measurements in 96 °C water without heating, for every tested velocity. Pertaining saturation temperatures can be determined from the line  $p_1 - p_{30}$  and plotted in diagram  $t-L$  to obtain line I between  $t_{1\ sat}$  and  $t_{30\ sat}$ . In the pressure range used, the saturation temperature is a linear function of pressure, thus, here line I is a

straight one but generally it is not and point by point construction is necessary. Now the position of  $B$  will be determined.

*b)* The increase of liquid temperature in the preheat section is supposed to be linear along the heating surface  $L$ . In the first approximation the measured mean heat flux is considered constant along the tube length  $L$ . Thus, if all the transferred heat is assumed to raise the liquid temperature we obtain a (fictive)  $t_{2*}$  at exit 2:

$$Q = w_F c_F (t_{2*} - t_1). \quad (5)$$

The straight lines II ( $t_1-t_{2*}$ ) and I intersect at point  $B$  in the  $t-L$  graph, which is marked in graph  $p-L$ , too.

In reality,  $q$  is not constant along the tube. In the vaporisation section the heat flux increases and only  $q_{\text{pre}}$  less than the mean  $\bar{q}$ , acts in the preheat section. If the difference is important, the slope of the preheat line I must be determined by trial and error. This can be done in 2 or 3 steps as follows. In fluid flow without change in phase the film coefficient is calculated from the Colburn equation [7]:

$$\frac{\alpha_{FO} D}{\lambda_F} = 0,023 \text{Re}_F \text{Pr}_F \left( \frac{\mu_b}{\mu_s} \right)^{0,14} \quad (6)$$

where  $\text{Re}_F$  refers to inlet conditions at 1. With  $\alpha_{FO}$  from (6) and mean fluid temperature  $\bar{t}_F$  from the previous approach we calculate  $q_{\text{pre}}$  and the new  $t_{2*}$ :  $\alpha_{FO} \cdot F_F (\bar{t}_s - \bar{t}_F) = q_{\text{pre}} \cdot F_F = w_F \cdot c_F (t'_{2*} - t_1)$  Line II' can be drawn, its intersection with line I gives point  $B'$ . If no further iteration steps are necessary, net vaporisation begins at this cross section.

*c)* In the vaporisation section the pressure drop is considered linear with  $L$ , thus it is represented by a straight line between  $B$  and  $p_3$  (found in boiling experiments). With pressures already known, local saturation temperatures are plotted in the  $t-L$  diagram (line III), which are the liquid temperatures as well, if liquid superheat is neglected.

The mean liquid temperature  $\bar{t}_F$  is obtained from the integral mean between  $t_1 - B' - t_2$  and the mean saturation temperature  $\bar{t}_{\text{sat}}$  between  $t_{1 \text{ sat}} - B' - t_2$ .

*1.3.2. Estimation of the mean wall temperature.* The heating surface is supposed to be clean at both steam and fluid side, without fouling or scale deposits. In that case the following equation holds (with mean values along  $L$ )

$$Q = \alpha_G \cdot F_G \cdot (t_G - t_{sG}) = \frac{\lambda_{\text{tube}}}{e} \left( \frac{F_G + F_F}{e} \right) \cdot (t_{sG} - t_{sF}) = \alpha_F F_F (t_{sF} - t_F) \quad (7)$$

From (7) both  $\bar{t}_{SF}$  and  $\alpha_F$  can be calculated if  $\alpha_G$  is known, as  $\lambda_{\text{tube}}$  and  $e$  are equipment constants.

To compute the condensing steam side film coefficient  $\alpha_G$  the Nusselt equation with modified factor was used [7]:

$$\frac{\alpha_G}{\lambda} \left( \frac{v^2}{g} \right)^{1/3} = 1,88 \text{Re}_K^{-1/3} \quad (8)$$

where the Reynolds number  $\text{Re}_K$  of the steam-condensate film was calculated with the measured amount of steam condensate and with physical properties at the mean film temperature (latter is determined by trial and error).

*1.3.3. Check of the calculation method.* The assumptions made for the calculation (film condensation of steam, no deposits on the heating surfaces) were verified by direct experiments. Cold water was circulated in the test tube and heated by steam under conditions inhibiting local boiling thus, Eq. (6) was valid for the liquid side film coefficient.

On the other hand the liquid side film coefficient could be taken from the measured transferred heat rate  $Q$  with Eq. (7) which gave the values  $Nu_{\text{meas}}$

Table I

Experimental data

No	$t_G$	$Q$	$q$	$t_1$	$t_4$	$\bar{t}_{SF}$	$\bar{t}_F$	$\bar{\delta}t_F$
	°C	$\frac{\text{kcal}}{\text{h}}$	$\frac{\text{kcal}}{\text{m}^2\text{h}}$	°C	°C	°C	°C	°C
$v_0 = 0.08 \text{ m/s}$								
				$w = 90 \text{ kg/h}$				
11	104.9	354	3760	99.9	100.0	104.0	100.97	3.03
12	105.1	340	3610	100.1	100.2	104.35	101.2	3.15
13	109.55	1750	18600	99.6	99.6	104.8	100.2	4.6
14	114.7	2690	28600	99.7	99.8	107.0	100.4	6.6
15	119.6	3875	41100	99.6	99.6	108.0	100.25	7.75
16	124.9	5145	54700	99.9	99.9	109.0	100.53	8.47
17	129.7	6350	67300	99.7	99.75	109.55	100.3	9.25
$v_0 = 0.36 \text{ m/s}$								
				$w = 405 \text{ kg/h}$				
21	104.4	600	6370	99.4	99.7	102.9	100.33	2.57
22	105.1	675	7170	100.1	100.3	103.95	101.0	2.95
23	109.55	1590	16900	99.6	99.6	105.25	100.6	4.65
24	114.7	2600	27600	99.7	100.0	107.4	100.8	6.55
25	119.5	3970	42200	99.5	99.7	107.6	100.65	6.95
26	124.9	5020	53300	99.9	100.1	109.4	101.05	8.35
27	129.7	6200	65900	99.7	99.8	110.1	101.0	9.1

to be compared with Eq. (6):

$$Nu_{\text{meas}} = A_{\text{meas}} Re_F^{0.8} Pr_F^{1/3} \left( \frac{\mu_F}{\mu_s} \right)^{0.14}$$

From 15 measurements ( $Re_F = 6000$  to  $80000$ ,  $\bar{t}_F = 20$  to  $85^\circ\text{C}$ ) we obtained for the mean

$$A_{\text{meas}} = 0.0242 \pm 0.0005 (\pm 2\%) = 1.051 \cdot 0.023 \pm 2\%.$$

The standard deviation of individual points was  $\sigma = \pm 0.0020 = \pm 8\%$ , which is a fairly good agreement for heat transfer measurements.

As the standard error of the mean value of  $A_{\text{meas}}$  ( $\pm 2\%$ ) is smaller than its deviation from the Colburn factor, this  $+5\%$  difference is significant and if it is not a consequence of individual features of our experimental apparatus then it means that *the calculation method described may involve  $+5.2\%$  error at maximum.*

#### 1.4. Experimental results

The measured data and values calculated from them are listed in Table I.

In the table the vapour content at the exit in points 2 and 3 is given in both weight and volume fraction. Vapour weight fraction is calculated from

$\alpha_F$	$\delta t_{\text{sat}}$	$P_1$	$P_1 - P_2$	$x_2$	$\eta_2$	$x_3$	$\eta_3$	Flow pattern
$\frac{\text{kcal}}{\text{m}^2 \text{h } ^\circ\text{C}}$	$^\circ\text{C}$	mm of $\text{H}_2\text{O}$	mm of $\text{H}_2\text{O}$	$\frac{\text{kg}}{\text{kg}}$	$\frac{\text{m}^3}{\text{m}^3}$	kg/kg	$\frac{\text{m}^3}{\text{m}^3}$	
$Re_0 = 5480$								
1240	1.4	12600	1623	0.0056	0.61	0.0067	0.67	plug flow
1150	1.55	12160	1623	0.0053	0.60	0.0064	0.62	plug flow
4050	4.0	10970	717	0.032	0.80	0.036	0.82	plug flow
4330	6.15	10960	665	0.055	0.85	0.055	0.85	plug flow
5300	7.4	10830	586	0.071	0.87	0.079	0.88	annular
6460	8.3	10880	532	0.105	0.89	0.106	0.90	annular
7300	9.0	10750	455	0.14	0.91	0.13	0.91	annular
$Re_0 = 24600$								
2500	—	11960	1652	0.0007	0.38	0.0018	0.46	plug flow
2430	—	12230	1652	0.0011	0.39	0.0022	0.50	plug flow
3630	3.3	11700	1363	0.0058	0.61	0.0065	0.62	plug flow
4210	5.45	11670	1259	0.010	0.68	0.011	0.69	plug flow
6030	6.0	11480	1125	0.0167	0.74	0.017	0.74	plug flow
6370	7.5	11560	1038	0.0215	0.77	0.022	0.77	annular
7240	8.3	11490	1000	0.0266	0.79	0.027	0.79	annular

Table I/2

No	$t_G$	$Q$	$q$	$t_1$	$t_4$	$\bar{t}_{SF}$	$\bar{t}_F$	$\bar{\delta t}_F$
		$v_0 = 0.63$ m/s		$w = 715$ kg/h				
31	105.0	835	8870	100.0	101.0	102.87	100.57	2.3
32	104.4	772	8200	99.4	100.4	102.35	99.95	2.4
33	109.55	1620	17200	99.6	99.9	105.1	100.58	4.5
34	114.65	2500	26600	99.5	100.2	107.5	100.93	6.57
35	119.5	3760	40000	99.5	100.1	108.4	101.21	7.2
36	124.96	4775	50700	99.9	100.6	110.3	101.8	8.4
37	129.7	5805	61600	99.7	100.6	111.5	101.6	9.8
		$v_0 = 0.77$ m/s		$w = 870$ kg/h				
41	104.7	826	8770	99.7	100.7	102.6	100.15	2.43
42	109.7	1703	18100	99.7	100.7	105.0	100.7	4.3
43	114.7	2580	27400	99.7	100.7	107.3	101.1	6.2
44	119.6	3800	40400	99.6	100.5	108.3	101.41	6.89
45	124.6	4900	52000	99.6	100.7	109.6	101.75	7.85
46	129.6	5770	61300	99.6	100.9	111.5	102.02	9.48

Table I/3

No	$t_G$	$Q$	$q$	$t_1$	$t_4$	$\bar{t}_{SF}$	$\bar{t}_F$	$\bar{\delta t}_F$
		$v_0 = 0.91$ m/s		$w = 1025$ kg/h				
51	105.0	1018	10700	100.0	101.0	102.3	100.5	1.8
52	104.4	944	10000	99.4	100.3	101.9	99.85	2.05
53	109.55	1841	19600	99.6	100.6	104.4	100.5	3.9
54	114.55	2670	28400	99.5	100.7	106.9	100.8	6.1
55	119.5	3860	41000	99.5	100.7	108.0	101.3	6.7
56	124.9	4850	51500	99.9	101.1	110.0	101.9	8.1
57	129.7	5745	61000	99.7	101.2	111.7	101.9	9.8
		$v_0 = 1.14$ m/s		$w = 1290$ kg/h				
61	104.9	987	10500	99.9	100.6	102.3	100.3	2.0
62	105.0	1073	11400	100.0	100.8	102.2	100.4	1.8
63	109.55	1970	20900	99.6	101.0	105.8	100.3	3.7
64	114.55	2880	30600	99.5	101.1	106.1	100.6	5.5
65	119.5	4070	43300	99.5	101.3	107.2	101.1	6.14
66	124.9	5060	53800	99.9	101.5	109.3	101.7	7.5
67	129.7	6053	64300	99.7	101.8	110.67	101.89	8.78

$\alpha_F$	$\bar{\delta}t_{sat}$	$P_1$	$P_1 - P_2$	$x_2$	$\eta_2$	$x_3$	$\eta_3$	Flow pattern
$Re_0 = 43600$								
3860	—	12430	1800	0	0	0	0.2	bubble flow
3440	—	12230	1800	0	0	0	0.2	bubble flow
3820	2.25	12200	1709	0.0017	0.44	0.0027	0.51	bubble flow
4040	4.7	12090	1567	0.0038	0.56	0.0046	0.58	plug flow
5550	5.78	12010	1452	0.0070	0.63	0.0079	0.65	plug flow
6020	7.2	12130	1400	0.0093	0.67	0.0101	0.68	plug flow
6260	8.4	12140	1416	0.011	0.70	0.012	0.70	plug flow
$Re_0 = 52900$								
3610	—	12450	1843	0	0	0	0	bubble flow
4200	1.7	12420	1795	0.0005	0.26	0.0018	0.46	bubble flow
4420	3.95	12430	1743	0.0022	0.48	0.0033	0.54	plug flow
5850	4.95	12430	1730	0.0045	0.58	0.0058	0.61	plug flow
6620	6.0	12490	1733	0.0063	0.63	0.0077	0.64	plug flow
6450	7.75	12560	1703	0.0078	0.65	0.0089	0.66	plug flow

$\alpha_F$	$\bar{\delta}t_{sat}$	$P_1$	$P_1 - P_2$	$x_2$	$\eta_2$	$x_3$	$\eta_3$	Flow pattern
$Re_0 = 62600$								
6000	—	12540	1835	0	0	0	0	} one phase liquid
4880	—	12340	1835	0	0	0	0	
5010	0.95	12490	1834	0	0	0.0007	0.33	bubble flow
4650	3.45	12450	1718	0.0010	0.38	0.0020	0.47	bubble flow
6080	4.4	12530	1735	0.0027	0.51	0.0038	0.56	bubble flow
6360	5.9	12740	1751	0.0043	0.57	0.0054	0.60	plug flow
6230	7.63	12750	1841	0.0057	0.61	0.0070	0.63	plug flow
$Re_0 = 78700$								
5240	—	12550	1856	0	0	0	0	} one phase liquid
6330	—	12690	1856	0	0	0	0	
5650	2.0	12640	1927	0	0	0	0	bubble flow
5560	2.3	12700	1854	0	0	0.0008	0.35	bubble flow
7040	3.1	12790	1820	0.00075	0.34	0.0018	0.46	bubble flow
7150	4.45	13070	1871	0.0015	0.44	0.0030	0.53	plug flow
7300	6.0	13030	1916	0.003	0.53	0.0044	0.58	plug flow

Table I/4

No	$t_G$	$Q$	$q$	$t_1$	$t_2$	$\bar{t}_{SF}$	$\bar{t}_F$	$\bar{\delta t}_F$
		$v_0 = 1.37$ m/s		$w = 1555$ kg/h				
71	104.9	1030	10680	99.9	100.5	102.2	100.2	2.0
72	105.1	1190	12650	100.1	100.8	101.9	100.3	1.61
73	109.5	2090	22200	99.6	100.9	103.6	100.2	2.35
74	114.5	3090	32800	99.5	101.4	105.5	100.5	5.02
75	119.6	4110	43600	99.6	101.6	107.2	100.9	6.3
76	124.9	5250	55800	99.9	102.0	108.6	101.5	7.14
77	129.7	6250	66400	99.7	102.3	109.9	101.7	8.25
		$v_0 = 1.62$ m/s		$w = 1855$ kg/h				
81	104.7	1095	11630	99.7	100.3	101.8	100.0	1.81
82	109.7	2150	22820	99.7	100.9	103.6	100.3	3.3
83	114.7	3300	35100	99.7	101.5	105.3	100.6	4.71
84	119.7	4260	45200	99.7	101.8	106.77	100.85	5.92
85	124.6	5250	55800	99.6	102.1	108.32	101.05	7.27
86	129.6	6445	68500	99.6	102.7	109.12	101.35	7.77

Table I/5

No	$t_G$	$Q$	$q$	$t_1$	$t_2$	$\bar{t}_{SF}$	$\bar{t}_F$	$\bar{\delta t}_F$
		$v_0 = 1.85$ m/s		$w = 2090$ kg/h				
91	104.7	1139	12100	99.7	100.2	100.68	99.95	1.73
92	109.7	2179	23150	99.7	100.7	103.56	100.2	3.36
93	114.7	3280	34850	99.7	101.3	105.05	100.5	4.55
94	119.7	4390	46600	99.7	101.7	106.36	100.75	5.61
95	124.6	5350	56800	99.6	102.0	107.97	100.9	7.07
96	129.6	6600	70100	99.6	102.6	108.57	101.2	7.37
		$v_0 = 2.08$ m/s		$w = 2345$ kg/h				
101	104.7	1160	12420	99.7	100.2	101.63	99.95	1.68
102	109.7	2240	23800	99.7	100.7	103.37	100.2	3.17
103	114.7	3350	35600	99.7	101.1	104.82	100.4	4.42
104	119.7	5440	48200	99.7	101.6	105.84	100.7	5.14
105	124.6	5605	59600	99.6	101.9	107.05	100.85	6.2
106	129.6	6825	72500	99.6	102.5	107.76	101.05	6.71

$\alpha_F$	$\bar{\delta}t_{sat}$	$P_1$	$P_1 - P_3$	$x_2$	$\eta_2$	$x_3$	$\eta_3$	Flow pattern
$Re_0 = 94800$								
5480	—	12660	1898	0	0	0	0	one phase liquid
7850	—	12610	1898	0	0	0	0	
6620	—	12700	1929	0	0	0	0	one phase liquid
6540	1.42	12800	1858	0	0	0	0	bubble flow
6930	2.75	12970	1915	0	0	0.0007	0.33	bubble flow
7800	3.44	13290	1897	0	0	0.0011	0.39	bubble flow
8100	4.75	13270	1937	0.00087	0.36	0.0022	0.49	bubble flow
$Re_0 = 111600$								
6420	—	12590	1848	0	0	0	0	one phase liquid
6830	—	12770	2018	0	0	0	0	
7210	1.26	12810	2141	0	0	0	0	one phase liquid
7660	1.87	13160	2197	0	0	0	0	bubble flow
7670	3.37	13240	2113	0	0	0.00067	0.32	bubble flow
8820	3.57	13530	2162	0	0	0.00095	0.37	bubble flow

$\alpha_F$	$\bar{\delta}t_{sat}$	$P_1$	$P_1 - P_3$	$x_2$	$\eta_2$	$x_3$	$\eta_3$	Flow pattern
$Re_0 = 127600$								
6955	—	12720	1929	0	0	0	0	one phase liquid
6885	—	12850	2047	0	0	0	0	one phase liquid
7645	0.35	13090	2182	0	0	0	0	one phase liquid
8320	1.31	13240	2213	0	0	0	0	one phase liquid
8050	2.77	13420	2234	0	0	0	0	bubble flow
9520	2.72	13580	2240	0	0	0	0	bubble flow
$Re_0 = 143400$								
7350	—	12900	1999	0	0	0	0	one phase liquid
7500	—	13100	2180	0	0	0	0	one phase liquid
8040	—	13170	2200	0	0	0	0	one phase liquid
9360	0.59	13350	2268	0	0	0	0	one phase liquid
9610	1.5	13470	2211	0	0	0	0	one phase liquid
10800	1.76	13660	2280	0	0	0	0	one phase liquid

the heat balance assuming thermal equilibrium in the vapor-liquid mixture. Volume fraction is determined from the calculated weight fraction by the Lockhart—Martinelli correlation, which accounts for the slip velocity between vapour and liquid phases (cf. Part II., Eqs (1), (2), (3)).

Flow patterns could be observed only at the exit from the test section with 1/1000 sec exposure photographs and 500 frame/sec speed motion pictures. According to these, flow pattern was dependent besides vapour quality

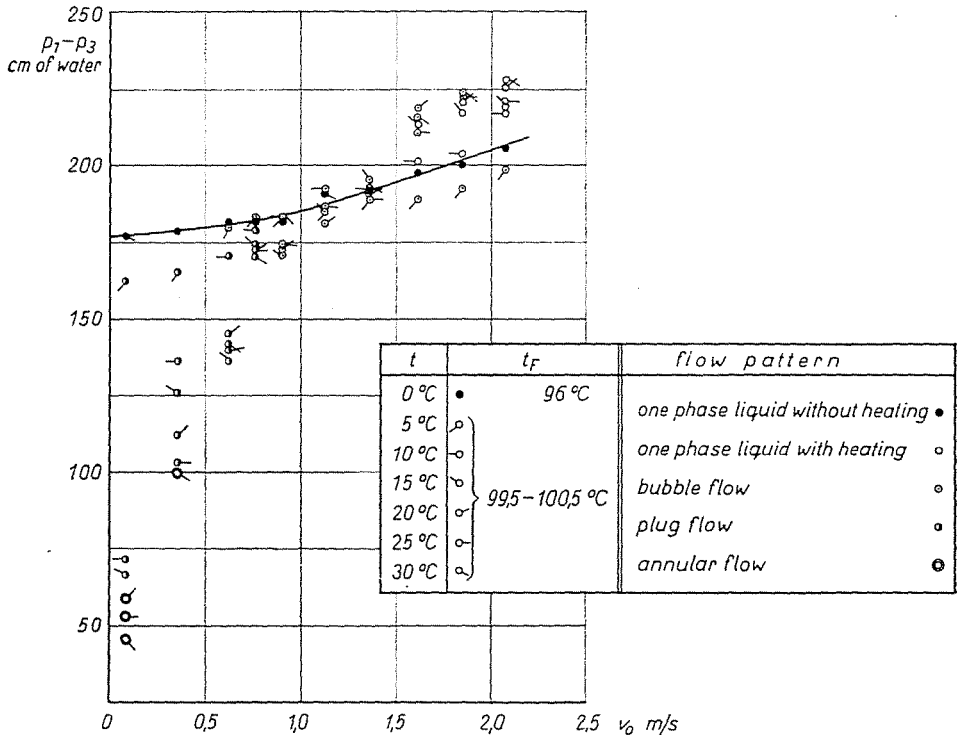


Fig. 5. Measured pressures in test tube vs. inlet velocity  $(p_1 - p_3) - v_0$ ; overall tube height 1780 mm, heated height 1500 mm

on mass flow rate too, e.g. by increasing the flow rate the regime of bubble flow extended towards both smaller and greater vapour contents. Thermal equilibrium existed only for quite low mass velocities: bubbles were visible in the sight glass even when the liquid was vapour free according to heat balance, if there was a possibility of subcooled boiling at the heating surface.

Fig. 5 shows the measured pressure difference between the inlet to the test section and the exit from the sight glass as a function of the inlet velocity. Exit flow pattern is indicated too. The pressure differences measured in 96 °C liquid without heating are plotted for comparison. With high exit vapour content (which is produced at a small inlet velocity and great temperature differ-

ence) pressure drop is under that measured in un-heated liquid. Evidently this is the working range for natural circulation (thermosyphon) evaporators (though all our experiments were made with forced circulation). The cause of the diminution of pressure difference is the decrease of the mixture density i.e. of the hydrostatic pressure.

With small vapour qualities (e.g. bubble flow) greater pressure differences were found than in unheated liquid because energy was consumed to accelerate the generated vapour. This is the typical operating range for forced circulation evaporators.

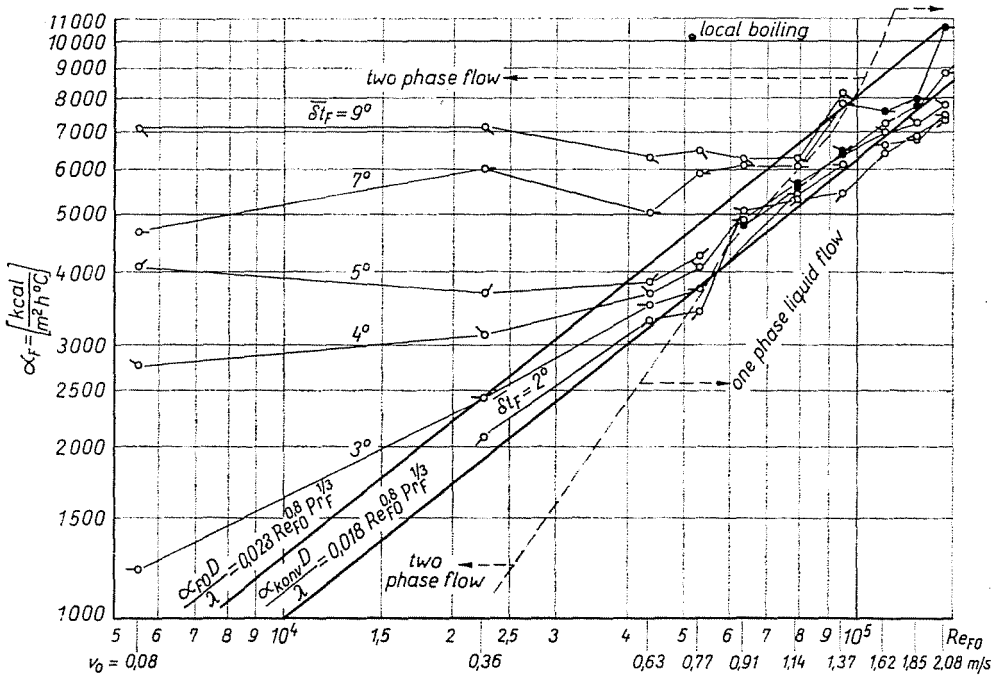


Fig. 6. Measured heat transfer coefficients compared with convective heat transfer

In Fig. 6 the film coefficient  $\alpha_F$  is plotted vs. the inlet velocity, and the inlet Reynolds number  $Re_{F0}$  with the temperature difference as parameter. Film coefficients expected on the basis of Eq. (6) are represented, too. It is remarkable that

1. in boiling experiments with high exit vapour content the film coefficient is little or not dependent on the inlet velocity, as expected upon results of previous investigators;

2. unexpectedly, however, in experiments with small or zero exit vapour contents lower film coefficients were found than given by the Colburn equation.

The factor in the Colburn equation is 0.023, from own measurements

with 96 °C water without boiling we determined  $0.0242 \pm 2\%$ , but from the boiling experiments (disregarded the results obtained with 5 °C overall temperature difference) it seems to approach the value 0.018. The deviation from the literature value is 22%, from own results (without boiling) 25%. Since a rigorous analysis of our experimental conditions showed that even in the worse case the error in the determined film coefficient is less than  $\pm 16\%$ , the above discrepancy cannot arise from experimental error and is to be regarded significant. This phenomenon is believed to be attributable to a "shadowing effect" of air bubbles absorbed in distilled water and now separating on the heating surface.

### Summary

Authors present an experimental procedure combined with calculation to determine heat transfer film coefficients in vertical tube evaporators. The calculation method renders the technically delicate wall temperature measurement superfluous, thus the determination of film coefficients can be accomplished also in industrial apparatus.

The experimental equipment was carefully built and by applying a compensation heat insulation the transferred heat could be measured accurately from independent steam- and heated-side heat balances. Pressure drop and heat transfer measurements were made in the operating range of both natural and forced circulation evaporators.

Prof. Dr. Károly TETTAMANTI }  
 Dr. Hajnalka HAJDÚ } Budapest XI., Műegyetem rkp. 3. Hungary

### Notations

$c$	specific heat, kcal/kg °C
$e$	tube wall thickness, m
$F$	heating surface, m <sup>2</sup>
$g$	acceleration of gravity, 9.81 m/s <sup>2</sup>
$L$	tube length, m
$p$	pressure
$Q$	heat transfer rate, kcal/h
$q$	heat flux, kcal/m <sup>2</sup> h
$r$	latent heat of evaporation, kcal/kg
$t$	temperature, °C
$v$	linear velocity, m/s
$v_0$	entrance velocity, m/s
$w$	mass flow rate, kg/h
$x$	vapor content, weight fraction, kg/kg
$\alpha$	film coefficient of heat transfer, kcal/m <sup>2</sup> h °C
$\lambda$	thermal conductivity, kcal/m h °C
$\eta$	volume fraction, m/m
$\mu$	dynamic viscosity, kg/m s
$\nu$	kinematic viscosity, m <sup>2</sup> /s
	Subscripts
BO	boiling
F	liquid
FO	all fluid is liquid

- G steam
- GK condensate of steam
- K condensate of vapor
- O entrance condition
- pre preheat section
- s surface
- sat saturation
- SF liquid-side surface
- SG steam-side surface
- v vapor
- 1, 2, 3, 4, 5 referring to Fig. 2
- Superscript
- average value

### References

1. AKIN, G. A., McADAMS, W. H.: *Ind. Eng. Chem.*, **31**, 483/491 (1939).
2. BERENSON, P. J., STONE, R. A.: *Chem. Eng. Progr. Symp. Ser.*, **61**, No 57 (1965).
3. BOARTS, R. M., BADGER, W. L., MEISENBURG, S. J.: *Ind. Eng. Chem.*, **29**, 912/918 (1937).
4. BORISHANSKI, W. M., KOZYREV, A. P., SVETLOVA, L. S.: *Konvektivnaia teploperedatsha w dvuchfaznom i odnofaznom potokach*. Izd. Energia, Moskva, 1964. pp. 71/104.
5. KIRSCHBAUM, E.: *Chem. Ing. Techn.*, **26**, 25/28 (1954).
6. KIRSCHBAUM, E.: *Chem. Ing. Techn.*, **33**, 479/484 (1961).
7. McADAMS, W. H.: *Heat transmission*. 3. Ed. McGraw-Hill, New York, 1954.
8. TOBILEVITSH, N. YU., EREMENKO, B. A.: *Gidrodinamika i teploobmen pri kipenii v kotlah vysokogo davlenia*. AN SSSR Moskva, 1955. pp. 187/205.